Climate Dynamics (2006) 27: 215–231
DOI 10.1007/s00382-006-0133-9

P. M. James

An assessment of European synoptic variability in Hadley Centre Global Environmental models based on an objective classification of weather regimes

Received: 13 June 2005 / Accepted: 6 February 2006 / Published online: 23 March 2006

Abstract The frequency of occurrence of persistent synoptic-scale weather patterns over the European and North-East Atlantic regions is examined in a hierarchy of climate model simulations and compared to observational re-analysed data. A new objective method, employing pattern correlation techniques, has been constructed for classifying daily-mean mean-sea-level pressure and 500 hPa geopotential height fields with respect to a set of 29 European weather regime types, based on the widely known subjective *Grosswetterlagen* (GWL) system of the German Weather Service. The objective method is described and applied initially to ERA40 and NCEP re-analysis data. While the resulting daily Objective-GWL catalogue shows some systematic differences with respect to the subjectively-derived original GWL series, the method is shown to be sufficiently robust for application to climate model output. Ensemble runs from the most recent development of the Hadley Centre's Global Environmental model, HadGEM1, in atmosphere-only, coupled and climate change scenario modes are analysed with regards to European synoptic variability. All simulations successfully exhibit a wide spread of GWL occurrences across all regime types, but some systematic differences in mean GWL frequencies are seen in spite of significant levels of interdecadal variability. These differences provide a basis for estimating local anomalies of surface temperature and precipitation over Europe, which would result from circulation changes alone, in each climate simulation. Comparison to observational re-analyses shows a clear and significant improvement in the simulation of realistic European synoptic variability with the development and resolution of the atmosphere-only models.

P. M. James
Hadley Centre for Climate Prediction and Research,
Met Office, FitzRoy Road, EX1 3PB, Exeter, UK
E-mail: paul.m.james@metoffice.gov.uk
Tel.: +44-1392-884262
Fax: +44-1392-885681

1 Introduction

The ability to simulate realistic synoptic-scale structure and variability over specific regions of the globe is a vital characteristic of climate models; necessary to ensure that predictions of climate changes, for example, are trustworthy and meaningful. To assess model performances in this area, an objective method for determining the nature of synoptic variability is required. Techniques that have been used frequently include cluster analysis (e.g. Maryon and Storey 1985; Corti et al. 1999) and empirical orthogonal function (EOF) analysis (e.g. North et al. 1982; Mo and Ghil 1987). Such methods yield sets of basic spatial patterns representing the most dominant modes of the variability. In the case of EOF analysis these are, by definition, orthogonal to each other and account for the maximum possible successive fractions of the total variance in the data. While this may be mathematically satisfying, the most significant EOFs tend to be rather predictable and inter-dependent (Horel 1981) and the individual patterns do not necessarily represent real synoptic structures. Furthermore, the EOFs are defined on the assumption that the patterns must be exhibited with both positive and negative sign, although no physical reason for this constraint may exist.

Although cluster analysis is somewhat less constrained, the cluster patterns which result vary according to the total number of desired clusters required and also tend to be large-scale, smooth structures which do not sufficiently capture real synoptic characteristics. Furthermore, some relatively infrequent but nevertheless significant synoptic types (especially those associated with blocking anticyclones over northern Scandinavia and the Norwegian Sea) do not normally appear in cluster analysis output.

Despite these limitations, such techniques can be useful for bringing out aspects of the variability in single

datasets. For comparison with the main findings of this paper, a set of EOF analyses of mean-sea-level pressure (MSLP) over Europe and the North Atlantic from NCEP re-analyses and from a set of climate model ensembles are compared in Fig. 1. The first three EOFs account for about 50% of the total variance but are typically quite close together in terms of their significance, notably in the re-analysis sets. Taken together, the first three EOFs clearly account for very similar variability patterns across all sets, but each set has superimposed these patterns in a somewhat different order and combination. For example, various combinations of EOF1 and EOF2 would be required to derive the classic North Atlantic Oscillation pattern, which does not appear automatically. The variance accounted for drops off quickly to EOF4 and then again to EOFs five and six (which typically account for about 6 and 5% of the variance, not shown), but these patterns are quite similar in all cases. Nevertheless, as these results highlight, each set yields generally somewhat different patterns, which may also be in a slightly different order. Hence, there is little else that can be achieved beyond an initial pattern comparison. Principal Component time series can be produced for each dataset and compared, but the patterns which these components refer to are never quite identical to each other. Clearly then, there would be advantages in having a fixed set of meaningful principal patterns to make comparisons with.

An alternative approach is thus to define a fixed set of typical weather patterns which recur from time to time and then classify the actual synoptic situation according to this set. A well-known system is Lamb's daily weather types (DWT) in which the basic flow direction and level of (anti)cyclonicity over the British Isles is determined on a daily basis (Lamb 1972). This system has since been automated by an objective method for the DWTs (Jones et al. 1993). A different objective classification method for the regional circulation type centred on Germany has been created by Bissolli and Dittmann (2001). However, a deficiency of both of these systems is that they are small in scale, only directly relating to circulation near to and over their respective regions and are not directly applicable to Europe as a whole.

A much more useful classification system, in this sense, is the *Grosswetterlagen* (GWL) catalogue, originally conceived by Baur et al. (1944), improved upon and later revised by Hess and Brezowsky (1952, 1969, 1977), recently updated by Gerstengabe et al. (1999) and since maintained by the German Weather Service (DWD), extending from 1881 to the present. Although the 29 *Hess and Brezowsky Grosswetterlagen* (HB-GWL) regimes have their primary focus on central Europe, they can also be viewed as readily identifiable large-scale circulation patterns involving most of Europe and the North-East Atlantic. Indeed their mean spatial scale is measurably larger than the DWTs, for example. Not only are the GWL patterns large in scale, but they also have a clear synoptic meaning in human terms, relating directly to the actual experience of weather spells in various parts of Europe. GWLs also have a longer temporal scale than the DWTs. Each GWL must last at least 3 days, so that transient patterns are classified either to belong within a long-lasting GWL type or to be the result of a transitory phase between two GWL types. Thus, GWLs represent regimes in the true sense of the word, rather than just a set of independent daily mean patterns.

Certainly, the GWL system is by no means perfect and has some deficiencies. In particular, weather types over the south-eastern and north-eastern corners of Europe are not very well separated by GWLs. Differing westerly types are perhaps not as well distinguished from each other as they could be, while some pairs of less common blocking types are very similar and could be effectively treated as one regime. However, for the greater part of Europe and its Atlantic seaboard, it is undoubtedly the best conceptual system currently available. The 29 GWL types are defined in Table 1, noting that the terms anticyclonic and cyclonic refer to the local bias over Central Europe within each clearly-defined large-scale pattern.

A problem with the official GWL catalogue is that it is a subjectively-assessed system which is likely to have some inconsistencies, especially in terms of when one GWL is deemed to have come to an end and the next started. The GWL catalogue is also rather inconsistent in the level of focus on the circulation directly over Central Europe. When this becomes too strong, the larger scale pattern may be incorrectly determined. It is therefore very hard to create an objective analysis method capable of reproducing it, and without an objective method, climate model simulations cannot be compared with observational datasets. Hence, there is a need for a re-assessment of the HB-GWL catalogue for the large-scale European circulation, based on consistent objective criteria.

In this paper, the performance of the Hadley Centre Global Environmental model, HadGEM1 (Martin et al. 2006), in simulating synoptic-scale variability specifically over Europe and the North Atlantic will be investigated. This model has been tested thoroughly in several different configurations and scenarios. Several ensemble integrations of the model have been performed in atmosphere-only mode, HadGAM1 (i.e. with no coupling to the ocean and prescribed sea-surface temperatures (SST) and sea-ice), at resolutions of N48 (2.5° latitude × 3.75° longitude) and N96 (1.25° latitude × 1.875° longitude), with 38 model levels in the vertical. In the fully coupled version at N96 resolution, extensive control integrations have been carried out using pre-industrial sea surface forcings and using historical time-varying anthropogenic forcings. The coupled control integration has also been used as a basis to compare equivalent integrations forced with double atmospheric CO_2 to investigate the nature of future climate change in the model.

In Sect. 2, the classification method for Objective-GWLs is outlined with a brief discussion of its properties

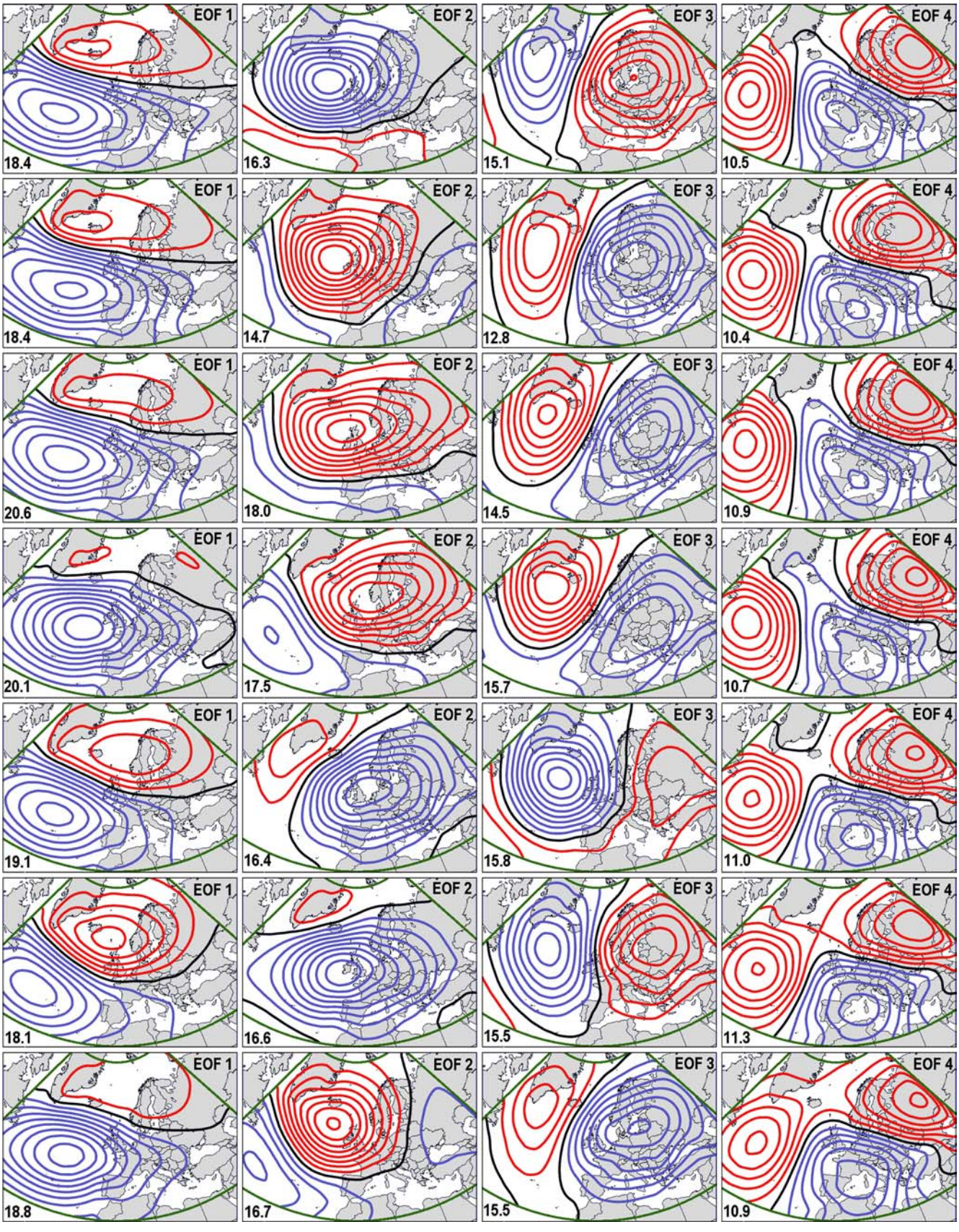
EOF 1
EOF 2
EOF 3
EOF 4
18.4
16.3
15.1
10.5
EOF 1
EOF 2
EOF 3
EOF 4
18.4
14.7
12.8
10.4
EOF 1
EOF 2
EOF 3
EOF 4
20.6
18.0
14.5
10.9
EOF 1
EOF 2
EOF 3
EOF 4
20.1
17.5
15.7
10.7
EOF 1
EOF 2
EOF 3
EOF 4
19.1
16.4
15.8
11.0
EOF 1
EOF 2
EOF 3
EOF 4
18.1
16.6
15.5
11.3
EOF 1
EOF 2
EOF 3
EOF 4
18.8
16.7
15.5
10.9

◀
Fig. 1 The first four empirical orthogonal functions (EOFs, *left to right*) resulting from EOF analyses of daily mean mean-sea-level pressure over the region indicated by the *green* boundary during the winter half-year, sinusoidally-weighted and centred on 15 January, for NCEP re-analysis data, 1948–2004, (*topmost*) and various climate model ensembles: HadAM3 N48/L19, HadGAM1 N48/L38, HadGAM1 N96/L38, HadGEM1 HistAnth, HadGEM1 Control and HadGEM1 2×CO_2 (*top to bottom*, respectively). The percentage of the total variance accounted for by each pattern is indicated at *lower-left* in each image. The grid-point values are normalized to total unity, such that the absolute contour values (red positive, blue negative) are irrelevant

and robustness. In Sect. 3, the method is applied to various model simulations and the statistics of the resulting Objective-GWLs are compared to those derived from re-analysed observational data. In Sect. 4, the mean circulation anomalies over Europe and the nearby Atlantic are determined for each set of models from their GWL statistics and used to estimate associated regional surface parameter responses. Finally, conclusions are drawn in Sect. 5.

2 Objective-GWL classification

The method used to construct an Objective-GWL catalogue has been described in detail by James (2006). Here, a summary of the method is presented. Based on HB's original concepts, the fields being used as the basis of the objective-GWL classification are Geopotential Heights at 500 hPa (GH500) and mean sea-level pressure (MSLP). These are calculated as daily mean fields at a 1°×1° resolution from the ECMWF ERA40 (Uppala et al. 2005) re-analysis dataset, covering the period September 1957 to August 2002. For each GWL type, climate mean composites of these fields are constructed, separate for winter and summer, based on the daily entries of the official HB-GWL catalogue. The year is split into equal halves and the compositing is undertaken with a sinusoidal weighting centred on mid-January and mid-July, respectively.

The analysis domain for the method is based on mean standard deviation fields of the 29 normalized GWL composite anomaly fields, which yields an estimate of where the GWL patterns are primarily significant. Within this domain, a circular nested domain is added, with a radius of 1,500 km centred on Central Europe. The latter gives a double-weighting to fields over this sub-region, because grid point values here are counted twice in the subsequent correlation analysis described further below. This improves the subjective quality of the results, given that most people view weather charts in a region-focussed way. The inner domain also enhances the method's ability to distinguish between cyclonic and anticyclonic bias over Central Europe itself—a key factor in the GWL system for separating neighbouring regimes. The chosen domains are illustrated in Fig. 2.

The resulting composite patterns represent well the nature of the different GWLs from a synoptic point of view. Although the subjectivity of the HB-GWL catalogue is problematical, over more than 40 years it has been possible to derive useful composite patterns which

Table 1 The 29 Grosswetterlagen with original German and translated English definitions

GWL	Original definition (German)	Translated definition (English)
01 WA	*Westlage, antizyklonal*	Anticyclonic Westerly
02 WZ	*Westlage, zyklonal*	Cyclonic Westerly
03 WS	*Südliche Westlage*	South-Shifted Westerly
04 WW	*Winkelförmige Westlage*	Maritime Westerly (Block E. Europe)
05 SWA	*Südwestlage, antizyklonal*	Anticyclonic South-Westerly
06 SWZ	*Südwestlage, zyklonal*	Cyclonic South-Westerly
07 NWA	*Nordwestlage, antizyklonal*	Anticyclonic North-Westerly
08 NWZ	*Nordwestlage, zyklonal*	Cyclonic North-Westerly
09 HM	*Hoch Mitteleuropa*	High over Central Europe
10 BM	*Hochdruckbrücke (Rücken) Mitteleuropa*	Zonal Ridge across Central Europe
11 TM	*Tief Mitteleuropa*	Low (Cut-Off) over Central Europe
12 NA	*Nordlage, antizyklonal*	Anticyclonic Northerly
13 NZ	*Nordlage, zyklonal*	Cyclonic Northerly
14 HNA	*Hoch Nordmeer-Island, antizyklonal*	Icelandic High, Ridge C. Europe
15 HNZ	*Hoch Nordmeer-Island, zyklonal*	Icelandic High, Trough C. Europe
16 HB	*Hoch Britische Inseln*	High over the British Isles
17 TRM	*Trog Mitteleuropa*	Trough over Central Europe
18 NEA	*Nordostlage, antizyklonal*	Anticyclonic North-Easterly
19 NEZ	*Nordostlage, zyklonal*	Cyclonic North-Easterly
20 HFA	*Hoch Fennoskandien, antizyklonal*	Scandinavian High, Ridge C. Europe
21 HFZ	*Hoch Fennoskandien, zyklonal*	Scandinavian High, Trough C. Europe
22 HNFA	*Hoch Nordmeer-Fennoskandien, antizykl.*	High Scandinavia–Iceland, Ridge C. Europe
23 HNFZ	*Hoch Nordmeer-Fennoskandien, zyklonal*	High Scandinavia–Iceland, Trough C. Europe
24 SEA	*Südostlage, antizyklonal*	Anticyclonic South-Easterly
25 SEZ	*Südostlage, zyklonal*	Cyclonic South-Easterly
26 SA	*Südlage, antizyklonal*	Anticyclonic Southerly
27 SZ	*Südlage, zyklonal*	Cyclonic Southerly
28 TB	*Tief Britische Inseln*	Low over the British Isles
29 TRW	*Trog Westeuropa*	Trough over Western Europe

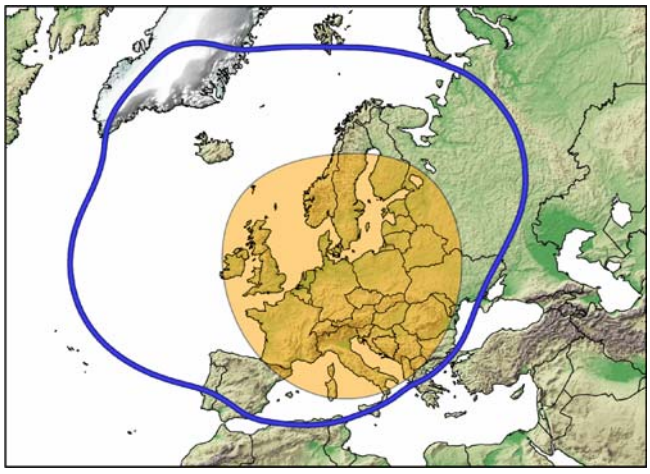

Fig. 2 Regions used for the objective-GWL analysis. The large domain is bounded by the blue contour; the inner domain is indicated by the *orange filled* area

span most of the typical synoptic variability that experience suggests is important. In Fig. 3, a 29-image panel shows the MSLP and GH500 mean composites for winter. The summer composites (not shown) are broadly similar, but are typically less intense, somewhat smaller in scale and exhibit some characteristic differences in form.

To calculate a daily Objective-GWL catalogue, 5-day running averages (with a 1–4-6-4-1 binomial filter) of the re-analysed or model data are made, thus smoothing out rapidly moving individual systems to enhance the correlation coefficients with the intrinsically smooth GWL composites. Mean pattern correlation coefficients between each GWL composite and the current MSLP and GH500 fields are derived and the GWL with the highest correlation is assigned for the given day. A GWL is always assigned in this way, no matter how low the highest correlation coefficient is. Finally, since each GWL event must last for at least 3 days, according to the original definitions, events lasting for only 1 or 2 days in the initial correlation calculations are filtered out and systematically replaced by the most appropriate alternatives, respectively, based on comparing relevant correlation values, applied successively in a sequence of logical steps. A list of these steps is not given here, however, as this would require considerable detailed explanation, inappropriate for this method summary.

While the above Objective-GWL method inevitably contains a certain unavoidable level of arbitrariness in setting the spatial domain and temporal filtering algorithms, once defined the method can be applied to many different datasets consistently. Hence, within the method's own framework, the resulting GWL catalogues are wholly objective. The method has been applied to both ERA40 and NCEP (Kalnay et al. 1996) re-analysis data over the 45 year period, September 1957 to August 2002, and the resulting catalogue compared to the original HB-GWL series. The NCEP data has a lower spatial resolution, 2.5°×2.5°, than ERA40. This results, for example, in a significant reduction in the number of cyclone tracks determined from NCEP data over the North Atlantic compared to ERA40 (Hanson et al. 2004). Otherwise, for dynamical fields such as MSLP and GH500, major differences between the re-analyses are not anticipated on the larger spatial scales important for the Objective-GWL pattern correlation method. The mean percentage of days with exact hits (days when the Objective-GWL and HB-GWL are the same) is 39.1% (ERA40) and 39.3% (NCEP). These values exceed 40% throughout the winter period from October to March, peaking in February at around 45%, while falling rather sharply in April (33%), May (34%) and August (35%).

These values may seem low at first sight. However, the HB-GWL catalogue is subjective and the assessments are unlikely to be entirely consistent over the years. There is also a large level of subjectivity about when one HB-GWL regime ends and another starts and the subjective GWL determination may misjudge the large-scale character of the regime if the focus on central Europe becomes too dominant. In any case, borderline cases which are close to two or more similar types are common and are hard to separate subjectively. Furthermore, the HB-GWL system allows for the possibility for defining an undefined (transitional) GWL on individual days, whereas the objective method does not.

To demonstrate that a significant proportion of the loss of exact hits is due to inconsistencies in the HB-GWL series, the newly-created Objective-GWL catalogue is used to generate a new set of composite patterns for each GWL and these are re-deployed, in turn, to construct a second version of the Objective-GWL catalogue, using the same methods as above. As a result of there being no remaining source of subjective error, the percentage of exact hits between these two objective series increases to nearly 80%. The remaining days on which a mismatch of GWL occurs is a measure of the fundamental limits of the method, caused by an inevitable loss of spatial accuracy due to binning into a finite number of patterns. Further tests have shown that the method loses approximately 4% of exact hits due to the logical temporal filtering—a formal necessity to ensure that all GWLs last at least 3 days. On the other hand, the 5-day binomial running filter increases the exact hits by about 6% by causing individual fields to resemble the smoothness of the GWL composites.

When comparing Objective-GWLs between ERA40 and NCEP, 92% of all days have exact hits. This is a very strong result, given the differences in resolution and the occurrence of borderline cases where very subtle differences could easily change the GWL-assignment, suggesting that the two re-analyses are practically interchangeable for the purposes of Objective-GWL classification. The differences between the Objective- and HB-GWLs are discussed further by James (2006), but

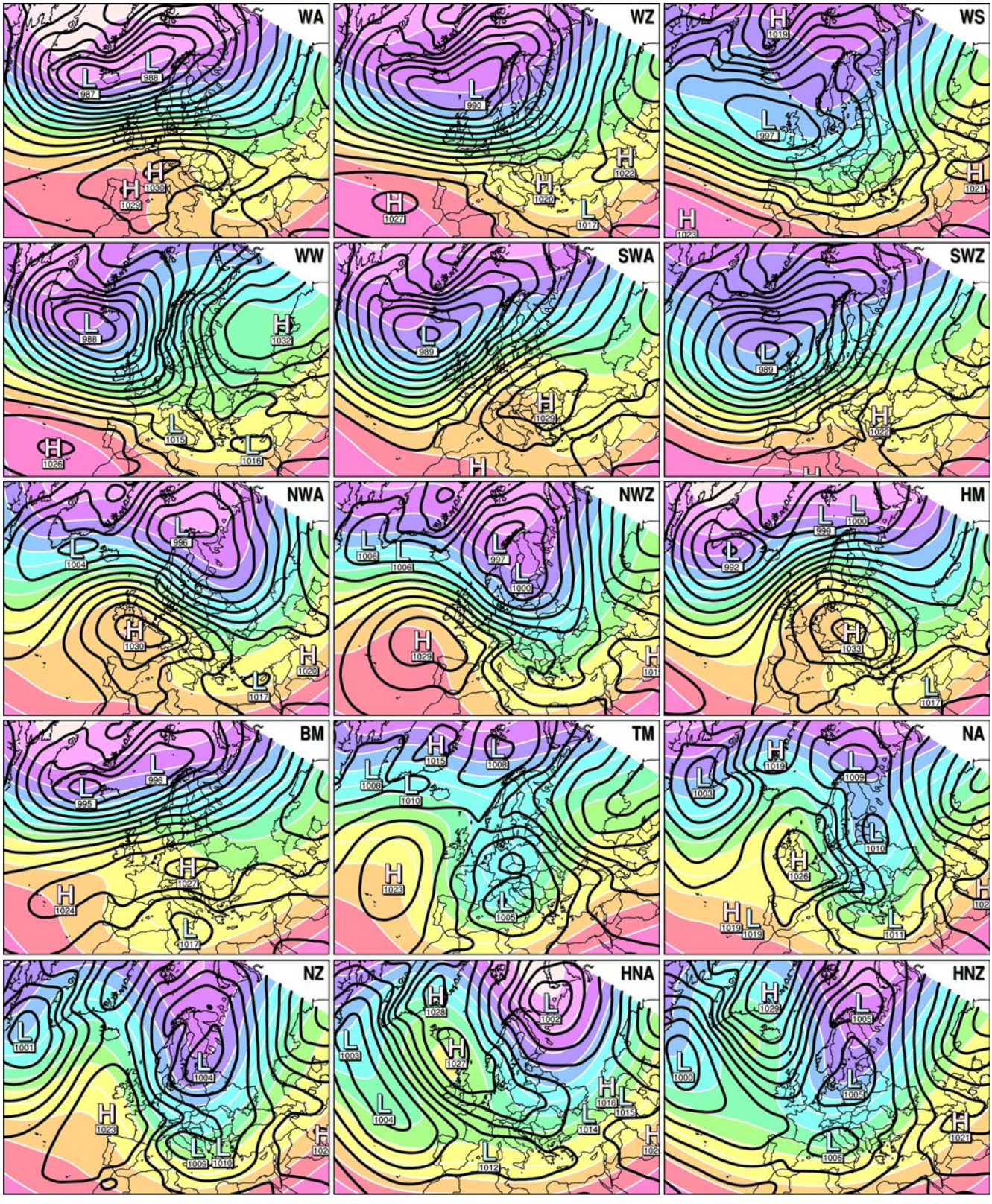

Fig. 3 a Climatological composites of GWLs 1-15 for the winter half-year, showing Geopotential height at 500 hPa (*colour-filled field*, contour interval 6 dam) and MSLP (*black contours*, interval 3 hPa, with plotted central pressure values with High, Low centre symbols). **b** Climatological composites of GWLs 16–29 for the winter half-year, showing Geopotential height at 500 hPa (*colour-filled field*, contour interval 6 dam) and MSLP (*black contours*, interval 3 hPa, with plotted central pressure values with High, Low centre symbols)

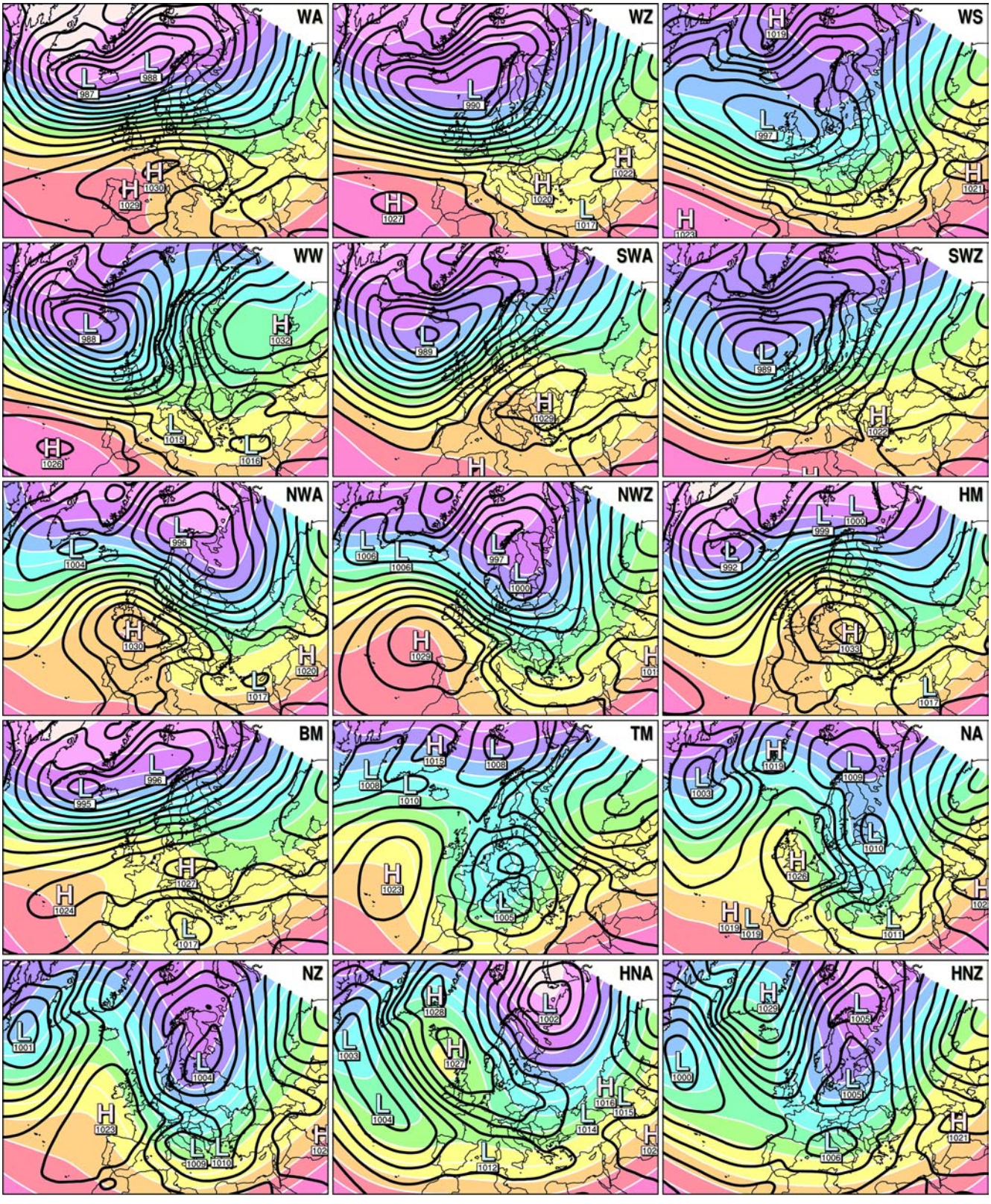

Fig. 3 (Contd.)

the purpose here of developing an objective GWL method is not to try to reproduce the HB-GWL catalogue itself, but to provide a robust basis set of weather patterns, which are meaningful synoptically and which can be calculated objectively from any equivalent dataset.

Table 2 The mean frequencies (percent × 10) of GWL events for NCEP re-analyses (three consecutive 17-year periods), ERA40 (two separate 17-year periods) and various climate model runs (sets of ensembles of 17-years width each), for (top) all year (centre) five winter months only, (bottom) five summer months only

	WA	WZ	WS	WW	SWA	SWZ	NWA	NWZ	HM	BM	TM	NA	NZ	HNA	HNZ	HB	TRM	NEA	NEZ	HFA	HFZ	HNFA	HNFZ	SEA	SEZ	SA	SZ	TB	TRW
Annual																													
NCEPRA-54-04	71	99	36	57	45	39	44	59	44	59	22	15	26	30	31	35	36	25	20	23	19	16	16	19	19	15	21	29	31
ERA40-62-78	67	103	30	45	43	38	47	56	44	57	19	14	24	30	38	30	38	24	27	20	28	13	19	20	27	13	23	27	36
ERA40-79-95	94	104	35	59	59	33	43	56	40	69	20	17	21	32	23	37	38	24	14	21	15	13	12	15	13	19	17	28	29
HadAM3-N48	49	85	60	92	33	46	23	37	34	39	40	18	18	19	36	20	35	17	26	17	42	23	32	18	32	17	24	42	27
HadGAM1-N48	69	103	49	58	23	40	59	71	27	55	30	17	31	27	46	26	36	18	34	16	21	14	23	12	15	10	16	29	24
HadGAM1-N96	71	100	39	65	32	42	57	64	33	60	21	13	33	32	33	34	39	20	24	19	21	17	13	13	17	15	17	31	25
HadGEM1-Ctl	70	93	30	52	44	44	67	59	40	76	15	9	30	35	33	31	32	13	15	17	18	20	15	18	18	16	24	31	35
HadGEM1-HAn	72	99	38	51	40	42	62	68	41	66	19	13	30	36	34	29	32	17	15	15	12	20	13	16	21	20	22	25	34
HadGEM1-CO_2	74	83	21	57	46	39	75	59	38	76	16	14	26	35	28	42	28	22	15	19	22	18	16	14	20	20	22	28	27
Winter (Nov–Mar)																													
NCEPRA-54-04	80	101	39	68	44	46	46	75	46	48	17	8	23	27	26	39	28	16	18	26	18	16	16	20	20	15	26	24	25
ERA40-62-78	63	93	35	54	38	53	60	72	40	43	19	5	29	24	35	32	37	12	17	24	19	17	23	23	34	13	28	30	26
ERA40-79-95	124	117	32	75	59	38	39	70	41	61	18	13	12	36	14	30	30	18	15	21	16	9	14	17	13	16	14	14	25
HadAM3-N48	56	113	74	105	44	63	22	58	41	24	31	15	21	14	30	16	25	19	23	17	13	15	16	10	24	16	23	47	23
HadGAM1-N48	86	144	82	26	54	51	76	38	40	24	19	28	13	22	17	25	18	40	21	12		9	18	6	10	7	16	19	9
HadGAM1-N96	81	150	44	82	38	55	55	75	42	41	18	14	26	16	18	29	28	15	24	21	16	9	12	11	11	16	18	26	10
HadGEM1-Ctl	80	129	36	72	64	63	56	61	54	51	10	5	22	23	18	23	23	12	14	21	14	14	9	11	18	22	26	26	20
HadGEM1-HAn	83	150	48	78	57	57	41	72	45	50	16	11	20	11	18	18	25	11	13	18	9	14	8	7	21	27	25	25	20
HadGEM1-CO_2	82	117	30	90	78	60	57	53	51	34	16	11	26	16	15	25	25	12	8	22	14	12	10	10	19	26	24	33	22
Summer (May–Sep)																													
NCEPRA-54-04	68	107	37	46	46	31	43	46	35	70	22	24	27	31	36	31	42	37	23	25	23	16	16	16	13	17	12	23	37
ERA40-62-78	72	125	32	42	43	28	33	36	23	80	13	25	22	34	37	27	29	44	34	22	46	8	18	14	16	13	13	19	51
ERA40-79-95	76	106	37	45	58	27	50	49	35	76	20	24	24	32	28	39	49	31	16	23	13	20	9	12	10	21	16	26	28
HadAM3-N48	47	63	54	78	20	33	25	25	22	53	50	21	14	20	43	19	53	17	31	18	79	21	43	18	35	15	13	37	31
HadGAM1-N48	63	65	27	24	17	29	77	70	17	75	33	14	37	39	72	37	43	19	28	12	31	16	22	18	17	13	15	31	37
HadGAM1-N96	72	66	34	38	25	31	66	61	30	82	21	13	37	44	47	41	47	21	21	17	27	24	13	14	18	12	15	28	36
HadGEM1-Ctl	75	74	24	28	26	29	86	64	27	108	17	14	36	48	45	40	38	13	17	9	21	26	18	17	9	9	15	26	41
HadGEM1-HAn	74	64	29	21	23	30	88	76	41	83	16	13	38	57	44	38	42	21	18	12	17	25	14	18	15	13	15	18	36
HadGEM1-CO_2	77	57	12	20	20	19	101	76	22	123	16	17	24	55	35	60	30	30	20	16	31	20	19	12	15	12	20	17	24

Table 3 95% confidence interval amplitudes (percent × 10) for the annual mean GWL frequencies given in Table 2 (top) for NCEP re-analyses, ERA40 and various climate model runs (as Table 2), based on calculating respective standard deviations of annual totals for all individual years

	WA	WZ	WS	WW	SWA	SWZ	NWA	NWZ	HM	BM	TM	NA	NZ	HNA	HNZ	HB	TRM	NEA	NEZ	HFA	HFZ	HNFA	HNFZ	SEA	SEZ	SA	SZ	TB	TRW
NCEPRA-54-04	10	10	7	8	8	6	8	9	7	7	5	4	6	5	6	5	7	5	5	5	4	4	4	4	6	4	5	6	6
ERA40-62-78	13	19	16	12	12	11	14	17	11	13	7	5	9	10	12	7	12	8	9	8	8	5	7	7	12	6	8	12	9
ERA40-79-95	20	17	10	14	18	10	16	14	9	16	6	8	8	9	9	8	13	6	7	8	8	5	7	5	6	8	8	9	11
HadAM3-N48	9	13	12	12	8	9	7	9	9	9	8	6	5	5	7	6	7	6	5	4	8	7	8	4	8	5	6	8	6
HadGAM1-N48	10	11	8	7	5	8	10	10	5	9	5	4	5	6	6	6	7	4	7	5	4	5	5	3	4	3	4	6	5
HadGAM1-N96	7	8	6	7	5	6	6	7	4	6	4	3	5	4	5	5	5	3	4	3	4	3	3	3	3	3	4	5	4
HadGEM1-Ctl	9	9	6	6	6	7	9	6	6	7	3	2	5	5	5	6	5	3	4	4	4	4	4	4	4	4	5	6	6
HadGEM1-HAn	9	10	7	7	7	6	7	8	6	8	4	3	5	6	5	5	5	4	3	4	4	4	3	4	5	4	4	5	5
HadGEM1-CO_2	7	9	5	9	6	6	8	7	6	8	4	4	4	6	5	6	5	4	3	4	5	4	4	3	4	4	4	4	5

The values shown are the amplitudes of any one side of the estimated error bars surrounding each mean, e.g. for NCEPRA-5404 WA has a mean of 7.1% and a confidence interval amplitude of 1.0%. Its confidence interval is therefore, $7.1 \pm 1.0\%$ such that its climate mean value has a likelihood of only 5% of falling outside of the range 6.1–8.1%

3 Objective-GWL statistics in Hadley Centre models

Now that a suitable objective method for assessing European synoptic variability has been established, it can be applied to various HadGEM1 ensemble sets. Comparison with re-analysed Objective-GWL statistics will then reveal the extent to which each model scenario is capable of generating a realistic spread of occurrence of weather regimes.

Under consideration of the availability of model run lengths during the early stages of this study, a period length of 17 years was chosen for the comparison. Five atmosphere-only (HadGAM1) ensemble simulations at N96 horizontal resolution and with 38 vertical levels have been performed. These integrations each cover at least the period, 1979 to 1995 inclusive, and have been forced with ancillary datasets, including observed sea-surface temperature (SST) and sea-ice fields, corresponding to that period. To test the direct effect of horizontal resolution, three equivalent ensemble runs of HadGAM1 have also been performed as above, but at N48. In addition, to examine the effect of general model development on the synoptic variability, two N48 integrations of the predecessor model, HadAM3, with 19 vertical levels, have been analysed. One of these HadAM3 runs used climatological SST and sea-ice fields, the other used time-varying SST and sea-ice, as with HadGAM1.

Much longer single integrations of the coupled model, HadGEM1, under different scenarios, have been performed. For the analyses here, four successive 17-year periods have been chosen, covering the period 1928 to 1995. The first set is based on time-varying Historical Anthropogenic (HistAnth) forcing ancillaries, including varying greenhouse gases corresponding to the above period. The second set is that of the HadGEM1 Control run, based on fixed pre-industrial forcing ancillaries for 1860. The final set is a climate change variant of the control run, in which atmospheric CO_2 is increased by 1% per annum from the start of the integration in 1860 onwards, and then held fixed at twice the present day values. This double CO_2 value is reached shortly after 1928, so that this set can be considered as a double-CO_2 basis for the purposes here.

To provide observational data for comparison, both NCEP and ECMWF re-analyses are used, noting that these are largely interchangeable for GWL statistics. Firstly, ERA40 data for the primary atmosphere-only period, 1979–1995, is taken. To estimate natural inter-decadal variability in the GWL statistics, the preceding 17 year period of ERA40, 1962–1978, was also examined. As will be shown, the low frequency variability is indeed substantial. Therefore, an extended re-analysis set using NCEP data is also examined, covering three successive 17-year periods, 1954–2004, which overlaps the given ERA40 periods almost equally at both ends.

Six-hourly MSLP and GH500 fields were extracted from each climate run and interpolated onto the same

1°×1° horizontal grid as the ERA40 fields had been, converted to daily-means and 5-day binomial running means formed. The NCEP re-analysis data is also interpolated in the same way onto the above grid. Although all of this data has a lower intrinsic resolution than ERA40, the temporal filtering and subsequent pattern correlations with smooth climate mean composite fields ensures that no systematic dependency on data resolution, within these bounds, is anticipated. The very high correspondence between GWL statistics for ERA40 and NCEP indeed shows this to be the case.

The total number of days of occurrence of each GWL in these runs is compared in Table 2 with totals for the re-analysis periods. To indicate their statistical significance, 95% confidence intervals have been calculated for the mean annual totals and are given in Table 3. As one would expect, these confidence intervals are widest where only one 17 year sequence is examined, as with the ERA40 periods, and narrowest where several 17 year ensembles are available, as with HadGAM1 N96, since the longer the time period analysed the lower the uncertainty in estimating climate means becomes. In general terms, all runs possess a quite realistic distribution of GWLs, with all 29 types occurring with a broadly realistic frequency. It is hard to spot any obvious systematic differences immediately. The most frequent types are the westerly regimes WZ and WA. In the annual mean, these appear with a similar frequency in all datasets, although WA is significantly less common in HadAM3 while WZ is less common in HadGEM1 2×CO_2, especially in summer. In general, WZ is more frequent in the models than in re-analyses in winter and less frequent in summer. Otherwise, the remaining less frequent regimes do not deviate significantly from observation in most cases. Comparison of Tables 2 and 3 reveals a small number of cases where the deviations are significant, but these do not warrant specific mention. In general, the greatest deviation from the re-analysed climate is seen with HadAM3, which has the lowest resolution and is the oldest model in development terms analysed here. In particular, regimes which feature localized Scandinavian blocking are more frequent (WS, WW, TM, HFZ, HNFZ significantly so), while opposing types are less common (WA, NWA, NWZ, BM, HNA and HB significantly so).

To test further how significant any differences in the frequency distributions between the models are, the mean frequency of each GWL per calendar month for any particular set have been correlated against those from each other set. This tests both the general GWL distribution across the 29 types as well as mean seasonal variations within each type. The respective correlation coefficients resulting from each set of 12×29 data point pairs are shown in Table 4.

When comparing with the 51-year NCEP dataset, the correlation coefficients show a very clear increase from HadAM3 N48/L19 to HadGAM1 N48/L38 and again from the latter to HadGAM1 N96/L38, confirming that advances in development and resolution of the atmosphere-only model have resulted in a measurable improvement in modelling European synoptic variability. The correlation coefficients are similar for HadGEM1 HistAnth and HadGEM1 Control to HadGAM1 N96, but drop slightly in HadGEM1 2×CO_2, suggesting that the climate change scenario has impacted on local synoptic variability, albeit only slightly.

When comparing the correlations between the two different ERA40 periods, the general model-to-model changes are similar to those above with NCEP. However, all models correlate better with the latter 1979–1995 period than with the 1962–1978 period. For the atmosphere-only models this might suggest that the modelled responses to 1979–1995 external constraints (such as SSTs) are closer to the 1979–1995 observed variability than to the observed variability of the earlier period. In other words, these models are responding in the correct sense to their external forcings. However, the HadGEM1 Control and HadGEM1 2×CO_2 simulations also exhibit this difference, even though they have constant pre-industrial forcing parameters, apart from CO_2 itself, so that one would not expect them to correlate better with either period from ERA40. Hence, this may indicate that the 1962–1978 period was rather unusual climatologically. Meanwhile, the correlations between either ERA40 set and NCEP are similar, suggesting in

Table 4 Matrix showing the mean correlation coefficients comparing respective climate-mean monthly GWL totals for various pairs of model/observational datasets, as labelled

	NCEPRA 54-04	ERA40 62-78	ERA40 79-95	HadAM3 N48	HadGAM1 N48	HadGAM1 N96	HadGEM1 HistAnth	HadGEM1 Control	HadGEM1 2×CO_2
NCEPRA-54-04	1.0000	0.8153	0.8546	0.5454	0.6832	0.7446	0.7429	0.7330	0.6800
ERA40-62-78	0.8153	1.0000	0.5592	0.4130	0.5182	0.5436	0.5841	0.5289	0.5341
ERA40-79-95	0.8546	0.5592	1.0000	0.4679	0.6209	0.6853	0.6873	0.6849	0.6357
HadAM3-N48	0.5454	0.4130	0.4679	1.0000	0.5687	0.5816	0.4813	0.5039	0.4506
HadGAM1-N48	0.6832	0.5182	0.6209	0.5687	1.0000	0.8796	0.8041	0.8442	0.7860
HadGAM1-N96	0.7446	0.5436	0.6853	0.5816	0.8796	1.0000	0.8598	0.8920	0.8231
HadGEM1-Ctl	0.7429	0.5841	0.6873	0.4813	0.8041	0.8598	1.0000	0.9035	0.8914
HadGEM1-HAn	0.7330	0.5289	0.6849	0.5039	0.8442	0.8920	0.9035	1.0000	0.8688
HadGEM1-CO_2	0.6800	0.5341	0.6357	0.4506	0.7860	0.8231	0.8914	0.8688	1.0000

Each correlation involves 29 GWLs × 12 months data points and indicates the similarity of both the distribution and seasonal cycle of GWL occurrence

turn, that the 1979–1995 period may also have been rather unusual, albeit very different from 1962 to 1978. These results highlight the need for long comparative data periods, due to the substantial levels of interannual and even interdecadal variability in GWL statistics.

When comparing the mean correlations between the various model sets and each other, the highest value is seen between the HadGEM1 HistAnth and Control runs, while the worst values all involve HadAM3. The results suggest that model resolution (both vertically and horizontally) has the most significant impact on the simulation of synoptic variability over Europe, whereas specific model details, even whether a coupled ocean is deployed or not, do not bring any further improvement. Nevertheless, the characteristics of each model set's differences in GWL distribution also need to be addressed. This is now the topic of the following chapter.

4 Estimating regional surface responses due to model circulation anomalies

Given that each model has a different GWL distribution from re-analyses, it is possible to use this information to estimate the expected anomalies of any particular parameter for each model based on their circulation anomalies alone. For example, an anticyclonic bias in summer over central Europe would be expected to result in a dry precipitation anomaly there and a warm anomaly in surface temperature on its western flank—i.e. this would be the anticipated GWL-bias in surface temperature due to circulation changes alone. Anticipated GWL-biases for any field are calculated by multiplying the mean GWL-frequency anomalies, relative to the 51-year NCEP re-analysis statistics, by the respective climatological GWL composites for that field, calculated from the full set of ERA40 data as described in Sect. 2.

This method is empirical in nature, since it does not take into account possible non-linearities in the amplitudes of the various regimes in each model, nor does it take possible systematic intra-GWL pattern biases into account. The latter, in particular, could have a significant impact if the typical synoptic patterns in a climate model were often markedly different to those observed in re-analyses. If this were so, they would not be well captured by the existing GWL patterns and the mean correlation coefficients with these patterns would be quite low. Furthermore, it would cast very serious doubt on the usefulness of the climate models at all. However, visual examination of many individual synoptic patterns occurring in the climate model outputs suggest that the model synoptic patterns are very similar in character to observed ones and are likely to be captured adequately by the existing set of GWLs. This is confirmed by computing the mean daily highest correlation coefficient between the daily synoptic patterns and each GWL for each model and re-analysis set. This gives a measure of how well the chosen GWL patterns model the actual synoptic patterns in each case. The values calculated show very little variation in general. For the re-analysis data the mean maximum coefficient is about 0.40, comparable to all N96 model sets which vary between 0.40 and 0.41, and is just slightly higher than for the N48 models at just under 0.39.

Hence, in spite of the potential issues above, the method is valuable because it provides an estimate of the likely direct effects of circulation biases on regional climate, independent of possible background effects introduced by the model physics as a response to anomalous forcing terms (especially in cases where an ambient local bias is known to be present). Indeed, the anticipated GWL-biases will be more indicative of the human experience of regional climate than actual mean anomaly fields would be, because the latter, which is standard validation output (i.e. model *minus* re-analysis), might itself mask significant non-linear effects.

To illustrate this point, an idealized but possible scenario is described. Suppose a model's cyclonic westerly flow in winter was often much stronger than the same type of flow in a re-analysis, while easterly circulation types were often weaker than they are the re-analysis. On the other hand, GWL statistics showed that cyclonic westerly types were less frequent than normal, while some easterly types were more common than normal. Thus, although these two aspects partially cancel each other out, this model could actually still have a resulting mean cyclonic westerly anomaly in its validated MSLP-minus-Re-analysis field. Normally, a warm bias over central and southern Europe would be expected from cyclonic westerly anomalies in winter. However, a strong westerly flow will *not* have a very different surface temperature signal from a weaker westerly flow, so the frequency of westerly flow events is likely to play a much bigger role than the circulation strength should do. In this example, the anticipated GWL-bias for surface temperature would pick up successfully the cold anomaly over central Europe, *despite* the mean MSLP anomaly showing a westerly bias in the same region.

The anticipated GWL-biases of the dynamical fields, MSLP and GH500, and the model-physics derived surface fields, daily mean 2 m temperature and daily total precipitation, all based on ERA40 GWL-composites, for the three atmosphere-only model sets, are shown in Fig. 4. As expected, HadAM3 has the strongest biases and exhibits a cyclonic bias centred near to the British Isles and an anticyclonic bias over north-west Russia, shifting over to Finland in summer. In winter, this results in a positive surface temperature anomaly over southern Europe of up to $+0.5$ K and a precipitation excess over south-western Europe of up to $+0.6$ mm/day, notably over the Atlantic coastlines of Iberia and France. Meanwhile, the easterly anomaly over Scandinavia introduces a cold bias of up to -0.5 K there and a dry anomaly centred over Norway of up to -0.4 mm/day. In summer, the peak anomalies are similar in magnitude, but the temperature response is reversed, becoming anomalously warm over Scandinavia and cold

over south-western Europe, due to the normal seasonal reversal of the mean land-sea temperature contrasts. The precipitation excess shifts to the Alpine region.

In HadGAM1, the GWL-bias patterns become slightly weaker and shift to the north and east. In winter, the cyclonic bias is centred over southern Scandinavia and most of mainland Europe has a warm anomaly. A cold anomaly remains in place over Scandinavia but this is weak at N96. There is a general precipitation excess across most of Europe north of the Alps, but Iberia and Mediterranean Europe is rather dry. In summer, a quite different average regime is present, with an anticyclonic bias centred to the north-west of the British Isles. The anomalous northerly flow results in a cold bias over much of mainland Europe, where it is also slightly wetter than in NCEP. The British Isles is affected most by the adjacent anticyclone and has a weak dry anomaly. The summer biases are generally weaker at N96.

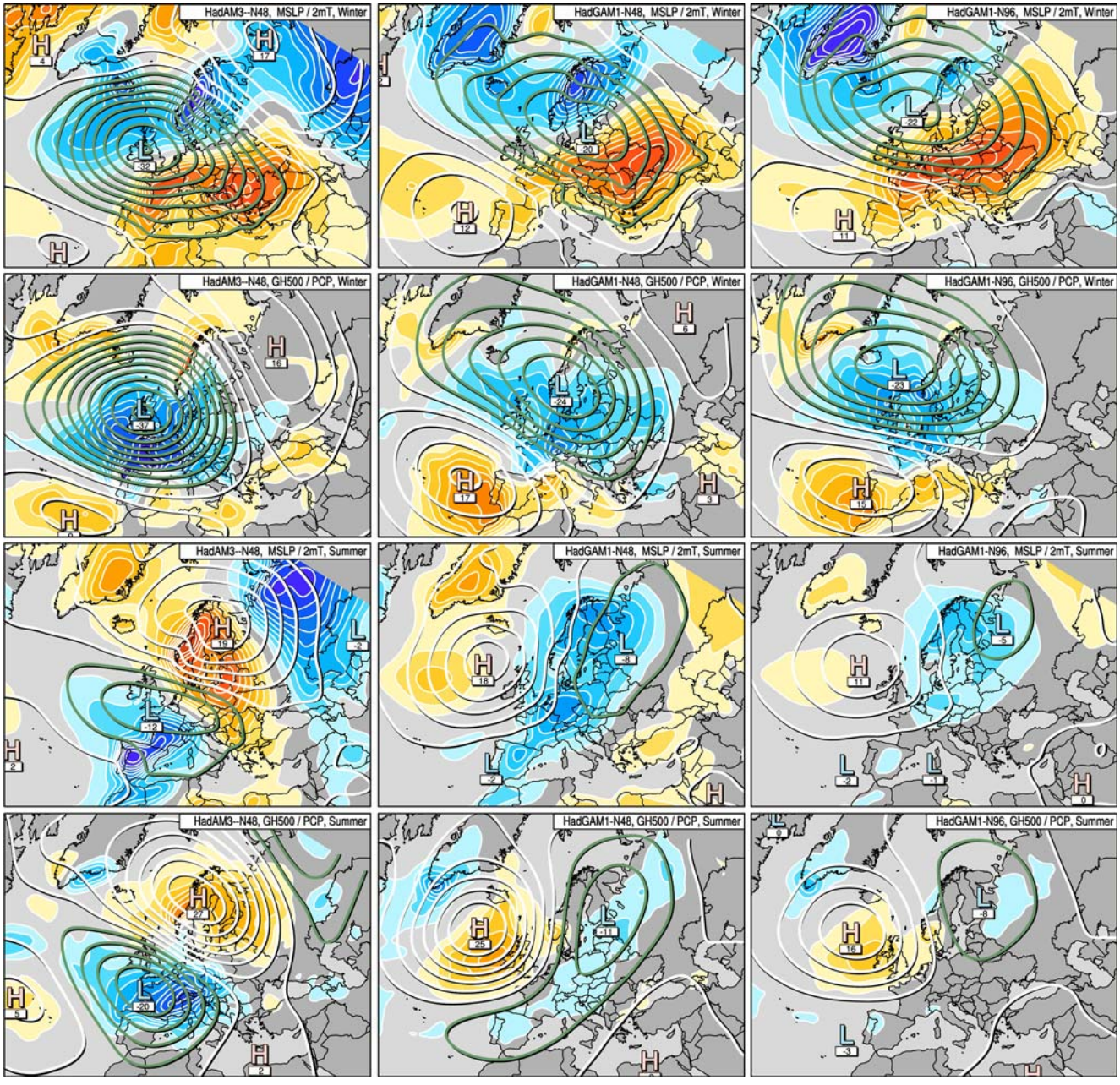

Fig. 4 Anticipated anomalies based on mean circulation changes derived from GWL statistics applied to GWL-composite fields calculated from ERA40 data, 1957–2002, of (rows 1 and 3) MSLP (contours, interval 0.4 hPa, negative contours are green, centres indicated in units of 0.1 hPa) with 2 m-temperature (*colour-fill*, interval 0.05 K, blues negative, reds positive) and (rows 2 and 4) Geopotential Height at 500 hPa (contours, interval 4 m, negative contours green; centres indicated in units of 1 m) with Precipitation (*colour-fill*, interval 0.05 mm/day, reds negative, blues positive), for three atmosphere-only sets: (*left*) HadAM3 N48/L19, (*centre*) HadGAM1 N48/L38 and (*right*) HadGAM1 N96/L38, for winter (*top half*) and summer (*bottom half*) half-years

Estimates of the anticipated circulation anomalies of the dynamical fields are included to show whether systematic biases like those described above might be present in any of the simulations, by comparing the GWL-derived anomalies with validated absolute MSLP and GH500 anomalies formed by subtracting re-analysed climate means from the respective model climate means; the latter being the standard method of validating a model's climate. Furthermore, any differences between the GWL-biases of near-surface temperature or precipitation and the respective model validation anomalies could be indicative of additional biases resulting from the associated model physics schemes.

The validated absolute anomalies of the four fields shown in Fig. 4 have been calculated for the three atmosphere-only models and are shown in Fig. 5. The absolute anomalies of the dynamical fields correlate to a certain extent with the GWL circulation anomalies, noting that a good correlation can only be expected within the broad region where the GWLs have their

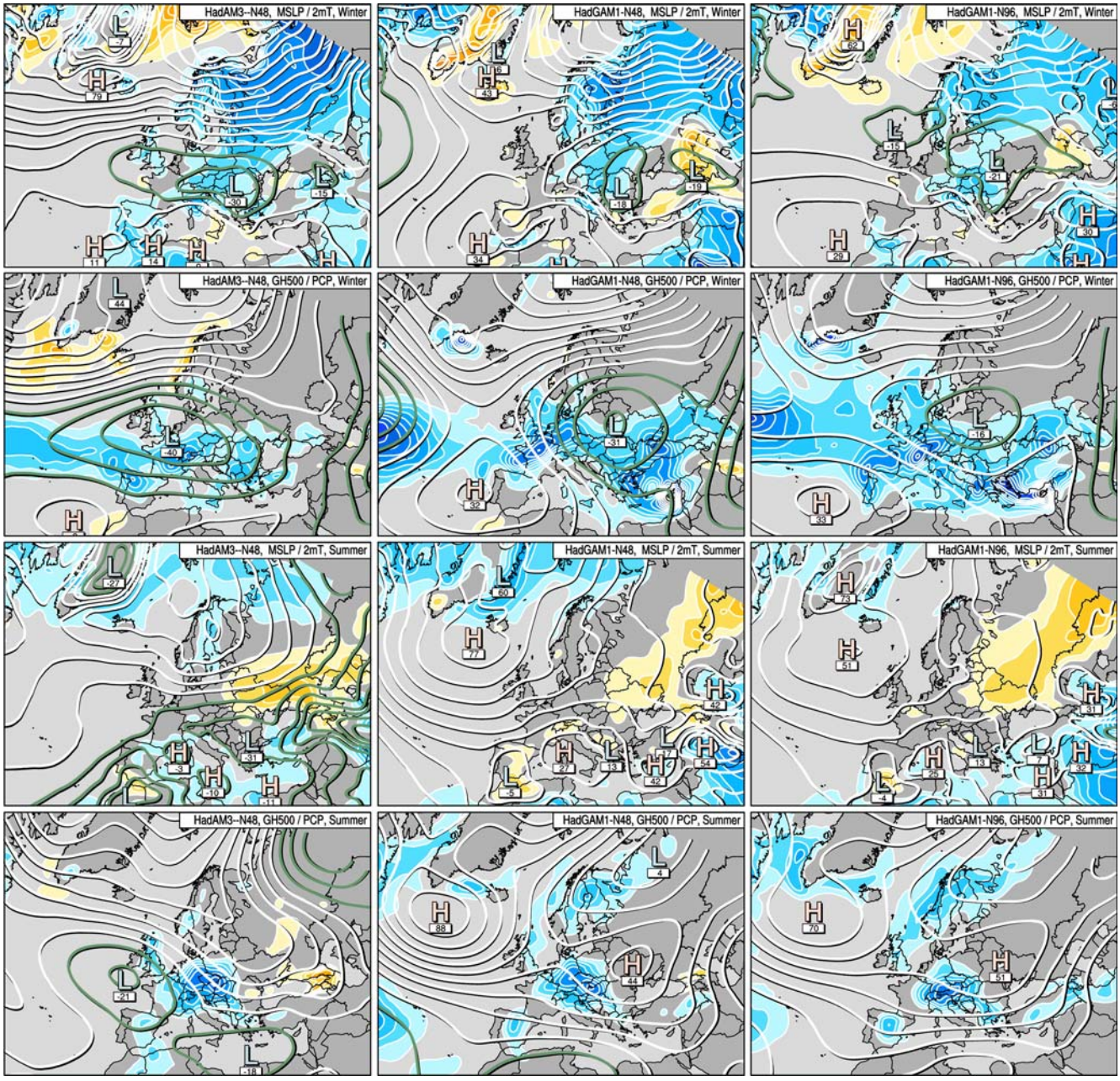

Fig. 5 Absolute anomalies, validated against ERA40 data for 1979–1995, of (rows 1 and 3) MSLP (contours, interval 1 hPa, negative contours are green, centres indicated in units of 0.1 hPa) with 2 m-temperature (*colour-fill*, interval 1 K, blues negative, reds positive) and (rows 2 and 4) Geopotential Height at 500 hPa (contours, interval 10 m, negative contours are *green*, centres indicated in units of 1 m) with Precipitation (*colour-fill*, interval 0.25 mm/day, reds negative, blues positive), for three atmosphere-only sets: (*left*) HadAM3 N48/L19, (*centre*) HadGAM1 N48/L38 and (*right*) HadGAM1 N96/L38, for winter (*top half*) and summer (*bottom half*) half-years

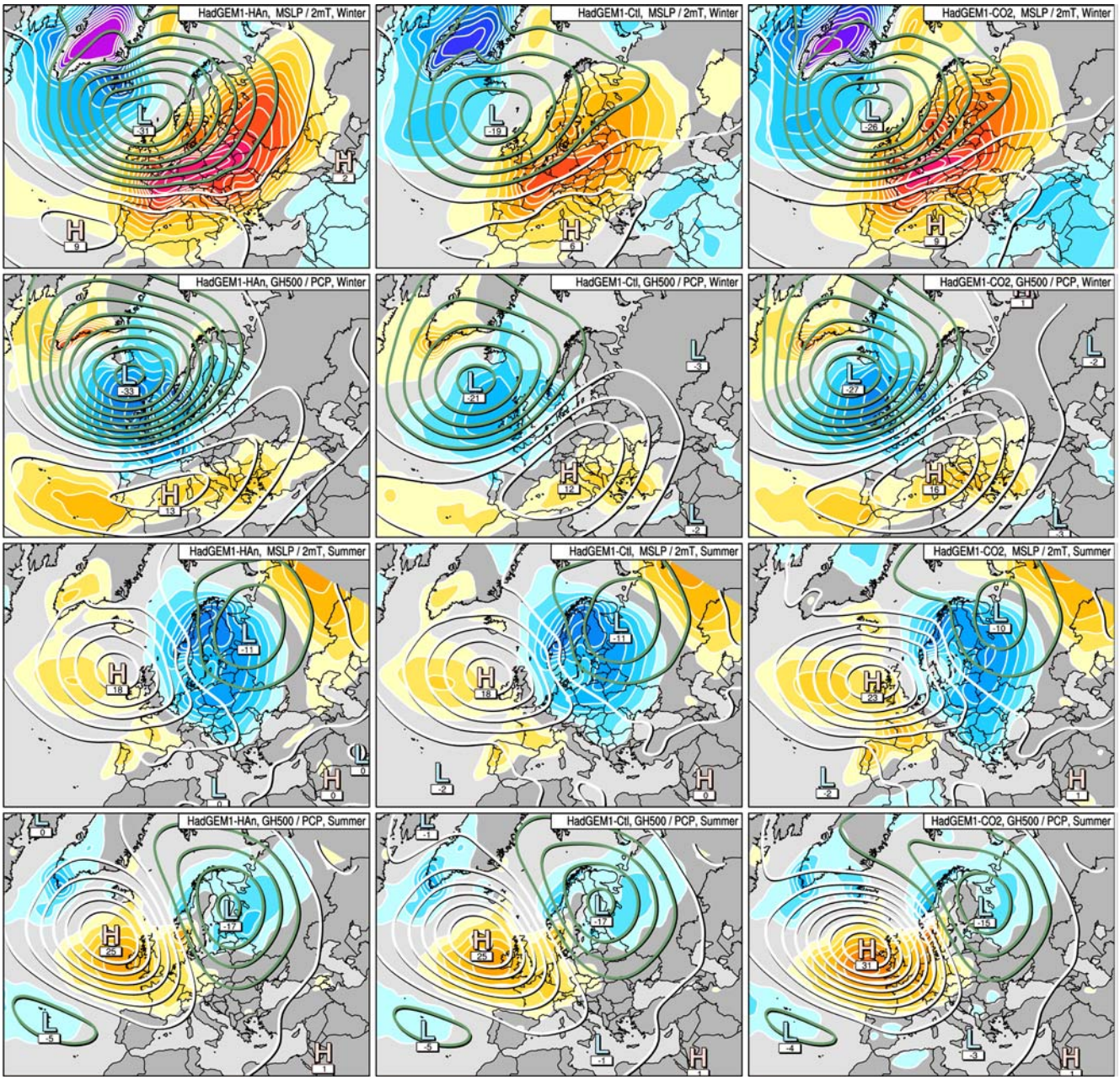

Fig. 6 Anticipated anomalies based on mean circulation changes derived from GWL statistics applied to GWL-composite fields calculated from ERA40 data, 1957–2002, of (rows 1, 3) MSLP (contours, interval 0.4 hPa, negative contours are green, centres indicated in units of 0.1 hPa) with 2 m-temperature (colour-fill, interval 0.05 K, blues negative, reds positive) and (rows 2, 4) Geopotential Height at 500 hPa (contours, interval 4 m, negative contours are green, centres indicated in units of 1 m) with Precipitation (*colour-fill*, interval 0.05 mm/day, reds negative, blues positive), for three HadGEM1 N96/L38 sets: (*left*) Historical Anthropogenic, (*centre*) Pre-Industrial Control and (*right*) Double CO_2 forcings, for winter (*top half*) and summer (*bottom half*) half-years

sphere of influence, approximated by the outer boundary in Fig. 2. Nevertheless, dominant large-scale biases are present which partly mask the circulation anomalies yielded by the GWL method. In particular, both MSLP and GH500 are generally higher in the models than in ERA40, especially in summer. The best correlation in winter is shown by HadGAM1 N96. For the other models, the nature of the differences do not suggest that any significant systematic biases are present, although cyclonic systems over central and north-west Europe may be slightly stronger than in ERA40, while anticyclonic systems in a similar location may be slightly weaker. In summer, differences in correlation quality between the models are not obvious and no clear systematic biases can be seen, noting that the weak cyclonic centres over north-east Europe in the GWL-derived

anomalies in HadGAM1 are on the edge of the region of GWL-influence and may be only an artefact of the dominant anticyclonic centres further west.

The validated absolute anomalies of the near-surface temperature and precipitation fields show much larger differences compared to the GWL-derived anomalies than the dynamical fields do. Indeed, it is rather difficult to relate the absolute anomalies here to their dynamical field equivalents. The temperature fields are derived from model output for the 1.5 m level. Although this is not exactly the same as the 2 m fields in ERA40, the fields will be sufficiently similar for at least a qualitative discussion. The absolute temperature anomalies are much larger than the GWL-derived anomalies, suggesting that substantial systematic biases are present in the models, albeit less so in the case of HadGAM1 N96. These are presumably related to aspects of the model's surface physics and how they compare to the physics in

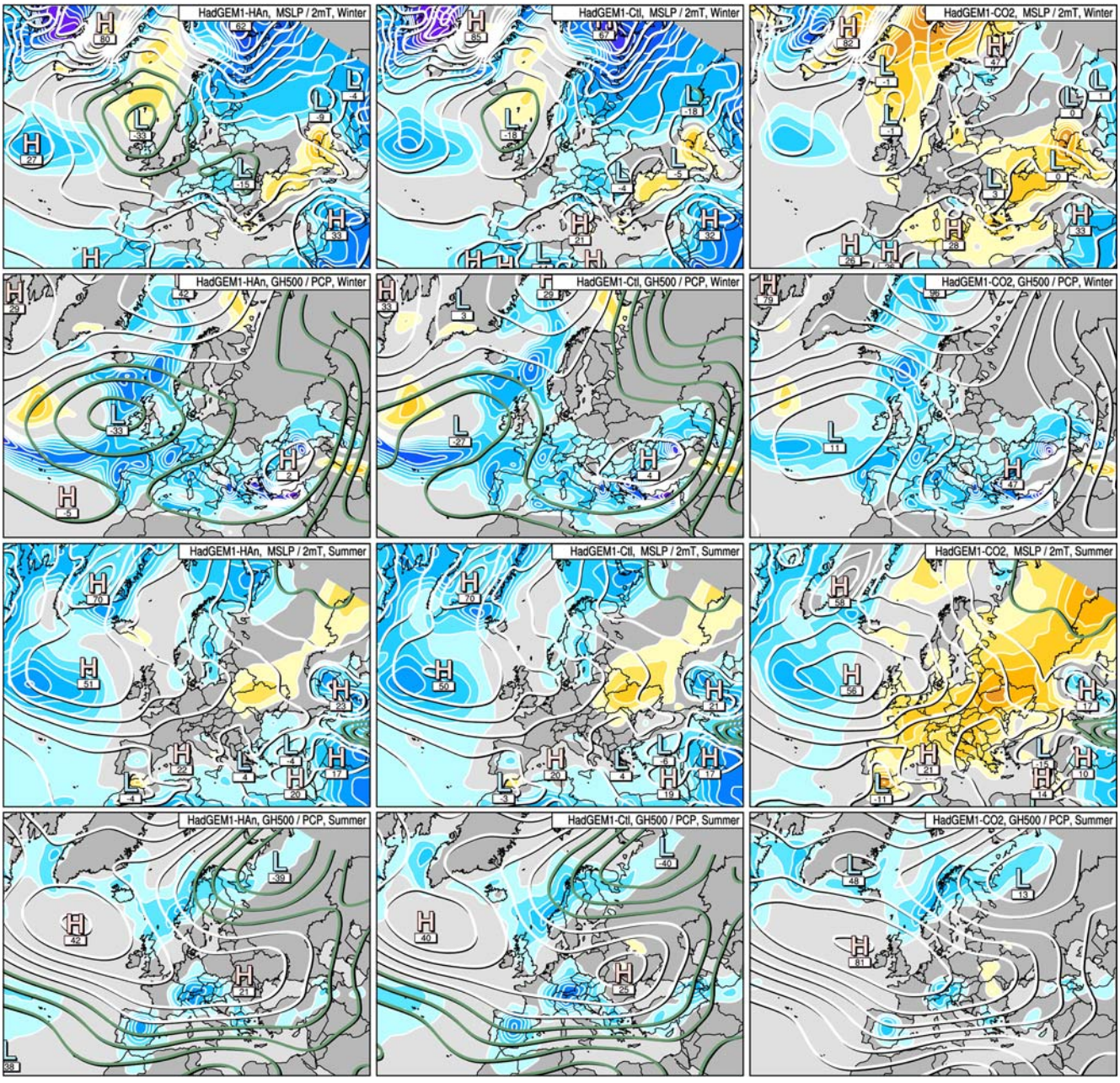

Fig. 7 Absolute anomalies, validated against ERA40 data for 1979–1995, of (rows 1 and 3) MSLP (contours, interval 1 hPa, negative contours are green, centres indicated in units of 0.1 hPa) with 2 m-temperature (*colour-fill*, interval 1 K, blues negative, reds positive) and (rows 2 and 4) Geopotential Height at 500 hPa (contours, interval 10 m, negative contours are green, centres indicated in units of 1 m) with Precipitation (*colour-fill*, interval 0.25 mm/day, reds negative, blues positive), for three HadGEM1 N96/L38 sets: (*left*) Historical Anthropogenic, (*centre*) Pre-Industrial Control and (*right*) Double CO_2 forcings, for winter (*top half*) and summer (*bottom half*) half-years

the ERA40 model, noting that Simmons et al. (2004) have shown that the ERA40 2 m temperature fields approximate area-averaged observed instrumental readings well, so that the magnitudes of the calculated GWL-derived temperature anomalies in Fig. 4 are probably quantitatively realistic. In winter, the models are rather cold over continental surfaces and rather warm over the sub-polar ocean. In summer, these biases largely reverse.

The validated absolute precipitation anomalies are also quite large and show generally higher precipitation than ERA40, especially in both HadGAM1 simulations. However, since it is known that ERA40's precipitation fields are generally rather poor (Brankovic and Molteni 2004) and probably underestimate precipitation in general, the anomaly values here are not important quantitatively and cannot be used to draw conclusions about model quality. Nevertheless, the comparison illustrates the difficulties that can arise when attempting to assess how mean circulation changes affect derived surface fields, based on validated absolute anomalies alone.

The anticipated GWL-derived circulation biases for the coupled model integrations are shown in Fig. 6 and compared to validated absolute anomalies in Fig. 7. HadGEM1 has a wintertime cyclonic bias over the north-western fringes of Europe, resulting in a south-westerly flow anomaly and a widespread positive surface temperature anomaly over virtually the whole of Europe which reaches up to $+0.7$°C over Germany. The precipitation bias is positive over north-western Europe and negative over the Mediterranean. In summer, the circulation bias is very similar to that in HadGAM1. There is surprisingly little difference between the circulation biases of the three HadGEM1 sets and even the double CO_2 set is similar, although the latter has the strongest summertime anticyclonic anomaly, which is shifted towards Ireland and results in a precipitation deficit over the British Isles of up to -0.4 mm/day.

Although the MSLP biases seem relatively small, the impact they have on the climate mean temperature and precipitation is locally quite significant. For example, a 0.4 mm/day loss in precipitation over the southern British Isles in summer represents approximately a 25% rainfall reduction, itself a very conservative estimate based as it is on the ERA40 precipitation climatology. As a climate mean this would lead to a significant increase in aridity, not to mention any potential changes to the occurrence of extremes in such a climate; the latter not being the subject of this paper, however. In general, the differences in the circulation biases between the HadGEM1 Control run and the HadGEM1 $2\times CO_2$ run are quite small and are not significant. Hence, even 68 years is clearly insufficient for estimating how a double CO_2 scenario would impact on the mean European circulation and its variability. A much longer period will need to be analysed to achieve this and will be the subject of a future paper.

The validated absolute anomalies of the dynamical fields in HadGEM1 correlate moderately well with the GWL-derived anomalies, while large-scale biases are seen which are quite similar to those in the atmosphere-only models. Systematic biases are weak, although the double CO_2 experiment has a relative anticyclonic bias in winter over much of Europe and a slightly weakened mean south-westerly flow anomaly, suggesting that its cyclonic centres to the north-west of Europe may be somewhat weaker than in present-day simulations. The surface temperature and precipitation absolute anomalies are broadly similar to those in the atmosphere-only models; except that the double CO_2 simulation has resulted in higher ambient mean surface temperatures. The latter highlights the advantages in using GWL-derived circulation anomalies in cases where ambient conditions are very different from climate normals.

5 Conclusions

The frequency and variability of persistent synoptic-scale weather patterns over the European and North-East Atlantic regions has been examined in a hierarchy of atmosphere-only and coupled climate model simulations. This study utilizes a new objective weather pattern classification method which is based on the widely known *Grosswetterlagen* (GWL) system of the German Weather Service. The method constructs a set of 29 weather patterns using ERA40 data and, subsequently, pattern correlations against these base patterns with temporal filtering techniques are used to generate a daily GWL catalogues from re-analysis data. Although the resulting daily Objective-GWL catalogue shows some systematic differences with respect to the subjectively-derived original GWL series, the method has sufficiently robust properties in its own right and can be applied meaningfully to climate model output.

Ensemble runs from the most recent development of the Hadley Centre's Global Environmental model, HadGEM1, in atmosphere-only, coupled and climate change scenario modes have been analysed with regards to European synoptic variability. At a general level, all simulations successfully exhibit a wide spread of GWL occurrences across all regime types. The variability of GWL occurrence on long time-scales (interannual and longer) in these simulations is high and is comparable to such variability in the re-analyses. These are very positive results in themselves, showing that the basic European modelled synoptic climate is realistic in both spatial and temporal senses.

Looking into more detail, however, various systematic differences in the mean seasonal distribution of some GWL types are seen in the different models. In winter, the atmosphere-only models typically have a cyclonic bias over western and central Europe, whereas the coupled models have a cyclonic bias to the north-west of the British Isles and an anticyclonic bias over the Mediterranean, leading to a south-westerly flow anomaly over central Europe. In summer all models have a consistent anticyclonic bias to the north-west of the

British Isles, leading to a northerly flow anomaly over central Europe. Such differences in mean GWL frequencies provide a very useful method for estimating local anomalies of derived surface parameters over Europe, such as surface temperature and precipitation, which would result from circulation changes alone, in each climate simulation. Geographically focussed signals resulting purely from local circulation anomalies can be seen very clearly using this method. On the other hand, standard absolute validation anomalies of surface parameters, relative to observational or re-analysed climate datasets, typically have ambient large-scale signals superimposed which mask any circulation related signals to a large extent. Although these may be important for assessing the performance of the model physics parametrisations, if the affect of circulation changes is the central theme to be studied, such standard validation methods are inadequate.

This study has also provided a first insight into potential changes in modelled European synoptic variability in relation to model development on the one hand and a climate change scenario on the other. A clear and significant improvement in the simulation of realistic variability with the development and increasing resolution of the atmosphere-only models, HadAM3 and HadGAM1, has been demonstrated. The most realistic climate was achieved with the HadGAM1 model at N96 horizontal resolution. It remains to be seen whether a further improvement might result when the planned higher resolution integrations are performed. For the coupled model simulations, HadGEM1, no significant changes were noted in a double CO_2 simulation compared to a control simulation. However, due to substantial interannual variability, it appears that a much longer period will need to be analysed before it will be possible to make robust statements about possible circulation changes over Europe in a changed climate.

Acknowledgements This work has been funded by the U. K. Government Meteorological Research programme. I would like to thank members of the Hadley Centre's climate modelling teams for their work in developing the HadGAM1/HadGEM1 models used in this study. In particular, the help and technical support of the Model Development and Evaluation group, Gill Martin, Mark Ringer, Chris Dearden, Christina Greeves and Tim Hinton, has been invaluable. The ERA40 and NCEP re-analyses were made available by the European Centre for Medium-range Weather Forecasts (ECMWF) and the National Centers for Environmental Prediction (NCEP) of the National Oceanic and Atmospheric Administration (NOAA), respectively, who are gratefully acknowledged. The German Weather Service is also thanked for providing the original *Grosswetterlagen* series and their work over the years in maintaining this valuable resource.

References

Baur F, Hess P, Nagel H (1944) Kalendar der Grosswetterlagen Europas 1881–1939. Bad Homburg (DWD)

Bissolli P, Dittmann E (2001) The objective weather type classification of the German Weather Service and its possibilities of application to environmental and meteorological investigations. Meteorol Z 10(4):253–260

Branković Č, Molteni F (2004) Seasonal climate and variability of the ECMWF ERA-40 model. Clim Dyn 22:139–155

Corti S, Molteni F, Palmer TN (1999) Signature of recent climate change in frequencies of natural atmospheric circulation regimes. Nature 398:799–802

Gerstengabe F-W, Werner PC, Rüge U (1999) Katalog der Grosswetterlagen Europas 1881–1998 nach P. Hess und H. Brezowsky. 5. Auflage. Potsdam Inst. für Klimafolgenforschung, Potsdam, Germany, pp

Hanson CE, Palutikof JP, Davies TD (2004) Objective cyclone climatologies of the North Atlantic—a comparison between the ECMWF and NCEP Reanalyses. Clim. Dyn 22:757–769

Hess P, Brezowsky H (1952) Katalog der Grosswetterlagen Europas. Berichte des Deutschen Wetterdienstes in der US-Zone, 33

Hess P, Brezowsky H (1969) Katalog der Grosswetterlagen Europas, 2. neu bearbeitete und ergänzte Aufl. Berichte des Deutschen Wetterdienstes 113. Offenbach am Main

Hess P, Brezowsky H (1977) Katalog der Grosswetterlagen Europas 1881–1976, 3. verbesserte und ergänzte Aufl. Berichte des Deutschen Wetterdienstes 113. Offenbach am Main

Horel JD (1981) A rotated principal component analysis of the interannual variability of the northern hemisphere 500 mb height field. Mon Wea Rev 109:2080–2092

James PM (2006) An objective classification method for Hess and Brezowsky Grosswetterlagen over Europe. Theor Appl Climatol (in press)

Jones PD, Hulme M, Briffa KR (1993) A comparison of Lamb circulation types with an objective classification scheme. Int J Climatol 13:655–663

Kalnay E et al (1996) The NCEP/NCAR 40-year re-analysis project. Bull Am Metrol Soc 77:437–471

Lamb HH (1972) British Isles weather types and a register of the daily sequence of circulation patterns 1861–1971. Geophys Mem Lond 116(4):85

Martin GM, Ringer MA, Pope VD, Jones A, Dearden C, Hinton TJ (2006) The physical properties of the atmosphere in the new Hadley Centre Global Environmental Model, HadGEM1. Part I: Model description and global climatology. J Clim (in press)

Maryon RH, Storey AM (1985) A multivariate statistical model for forecasting anomalies of 1/2-monthly mean surface pressure. J Climatol 5:561–578

Mo KC, Ghil M (1987) Statistics and dynamics of persistent anomalies. J Atmos Sci 44:877–901

North GR, Bell T, Modeng F, Cahalan RF (1982) Sampling errors in the estimation of empirical orthogonal functions. Mon Wea Rev 98:699–706

Simmons AJ, Jones PD, Bechtold VD, Beljaars ACM, Kallberg PW, Saarinen S, Uppala SM, Viterbo P, Wedi N (2004) Comparison of trends and low-frequency variability in CRU, ERA-40, and NCEP/NCAR analyses of surface air temperature. J Geophys Res 109:D24 DOI 10.1029/2004JD005306

Uppala SM et al (2005) The ERA-40 reanalysis. Q J Roy Met Soc 131:2961–3012